P-24

NASA CASE NO. LAR 14815-1-CU

PRINT FIG. 1

NOTICE

The invention disclosed in this document resulted from research in aeronautical and space activities performed under programs of the National Aeronautics and Space Administration. The invention is owned by NASA and is, therefore, available for licensing in accordance with the NASA Patent Licensing Regulation (14 Code of Federal Regulations 1245.2).

To encourage commercial utilization of NASA-owned inventions, it is NASA policy to grant licenses to commercial concerns. Although NASA encourages nonexclusive licensing to promote competition and achieve the widest possible utilization, NASA will provide the necessary incentive to the licensee to achieve early practical application of the invention. Address inquiries and all applications for license for this invention to **NASA Patent Counsel, Langley Research Center, Code 143, Hampton, Virginia 23665-5225.**

Serial No.: 07/820,432
01-03-92

LaRC

(NASA-Case-LAR-14815-1-CU) AERODYNAMIC DESIGN OPTIMIZATION USING SENSITIVITY ANALYSIS AND COMPUTATIONAL FLUID DYNAMICS Patent Application (NASA) 24 p

N92-29830

Unclas
G3/34 0111107

NASA Case No. LAR 14815-1-CU

AWARDS ABSTRACT

AERODYNAMIC DESIGN OPTIMIZATION USING SENSITIVITY ANALYSIS AND COMPUTATIONAL FLUID DYNAMICS

An efficient aerodynamic shape optimization method based on a computational fluid dynamics/sensitivity analysis algorithm has been developed which determines automatically the geometrical definition of an optimal surface starting from any initial arbitrary geometry. This method is not limited to any number of design variables or to any class of surfaces for the shape definition.

The novelty of this invention is found in determining the optimal aerodynamic surface for a given set of parameters and constraints using a minimum number of computational fluid dynamics analyses.

Inventors:	Oktay Baysal	Mohamad E. Eleshaky
Address:	1346 Brunswick Avenue Norfolk, VA 23508-1345	18-D Elizabeth Road Hampton, VA 23669
	ss: [redacted]	ss: [redacted]
Employer:	Old Domion University Research Foundation	
Evaluator:	David S. Miller	

Serial No.: 07/820,432
Filed: January 3, 1992

AERODYNAMIC DESIGN OPTIMIZATION USING SENSITIVITY ANALYSIS AND COMPUTATIONAL FLUID DYNAMICS

Origin of the Invention

The invention described herein was made in the performance of work under NASA Grant No. NAG-1-1188. In accordance with 35 U.S.C. 202, the grantee elected not to retain title.

Background of the Invention

1. Technical Field of the Invention

The present invention relates generally to designing aerodynamic shapes, and more particularly to the optimization of aerodynamic shapes using sensitivity analysis and computational fluid dynamics.

2. Discussion of the Related Art

Aerodynamic shape optimization has recently become a subject of considerable interest. This field of study involves the ability to determine the geometry of an aerodynamic configuration that achieves specified objectives subject to certain constraints and satisfies the governing equations of its flowfield. For instance, in attaining the geometry of an optimum airfoil section two basic categories of design methods exist.

The first category includes the inverse design methods, in which one specifies the surface pressure distribution and the method calculates the corresponding airfoil geometry. Examples of this approach include the hodograph methods which solve the linear potential equations in the hodograph plane, and a method which treats the two-dimensional flow as a set of streamtubes coupled through the position of, and pressure at, the stream

interfaces. The latter method solves the Euler equations which guarantees a proper treatment of shocks. Some of these methods have recently included the viscous effects through a coupled integral boundary layer analysis.

The second category includes the numerical optimization methods, which couple a flowfield analysis algorithm with an optimization algorithm. The aerodynamic quantities such as lift, drag, pitching moment, and pressure distribution are computed by the flowfield analysis algorithm for a certain configuration and are used in defining an objective function to be minimized or maximized. This objective function must relate changes in geometry to improvements in the aerodynamic quality of the design.

These methods require a significant level of experience and skill to define the geometrical aerodynamic shapes.

It is accordingly an object of the present invention to design an aerodynamic shape which maximizes performance within specified aerodynamic and geometrical constraints.

It is another object of the present invention to determine the unique aerodynamic shape which maximizes performance within specified aerodynamic and geometrical constraints regardless of the initial shape chosen to optimize.

It is another object of the present invention to achieve the foregoing objects with a process which does not require a complete computational fluid dynamics analysis of the shape as part of every iteration.

It is yet another object of the present invention to accomplish the foregoing objects in a simple manner.

Additional objects and advantages of the present invention are apparent from the drawings and specification which follow.

Summary of the Invention

According to the present invention, the foregoing and additional objects are obtained by choosing a function to optimize, determining a set of physical constraints, a set of constant design parameters and a set of variables which

may be modified to optimize the function. An initial shape must also be chosen, although the result is not dependent on this initial shape as this process determines the unique optimal shape. The constraints are analyzed to determine what the feasible space is, i.e. what ranges must each variable is limited to and an initial value for each variable is chosen within this feasible space. A complete computational fluid dynamics analysis is performed for the initial shape, the initial set of constant design parameters and the initial set of variables. The sensitivity coefficients for the initial shape and variables are calculated and the function is evaluated for the initial set of variables, ensuring that none of the constraints are violated. Based on the evaluation of the function, it is determined whether one or more than one variable will be changed. If one variable is changed, it is changed less than about 5% and the shape is redefined based on this change. An approximate flow analysis for the redefined shape is performed based on the sensitivity coefficients previously calculated. The function is evaluated for the new variables, ensuring that none of the constraints are violated and the redefined shape is evaluated to determine if the shape is optimal. If more than one variable is changed, the shape is redefined based on these changes and a complete computational fluid dynamics analysis is performed for the redefined shape. The function is evaluated for the new variables, ensuring that none of the constraints are violated and the redefined shape is evaluated to determine if the shape is optimal. These steps are repeated until the shape is optimal. Once the optimal shape is obtained, the shape may be evaluated to determine the sensitivity of the shape with respect to one or more of the design parameters.

Brief Description of the Drawings

Fig. 1 is a flow chart showing the overall design optimization process;

Fig. 2 is a flow chart showing the details of the direct method of the sensitivity analysis process; and

Fig. 3 is a flow chart showing the details of the adjoint variable method of the sensitivity analysis process.

Detailed Description of the Invention

The overall process of aerodynamic design optimization consists of the computational fluid dynamics analysis, the sensitivity analysis, the approximate flow analysis and the optimization method. A flow chart of the process is presented in Fig. 1. The following example illustrates this process.

Example

It is desired to determine the angles of the nozzle ramp, α, and of the cowl, β, that yield a maximum axial thrust force coefficient, F, subject to constraints, G_j. The angles α and β are the design variables, $\bar{X}_D$, and therefore, the number of design variables, NDV, is equal to two.

Mathematically, it is required to get

$$\max F(\bar{Q}(\bar{X}_D),\bar{X}_D) \tag{1}$$

$$G_j(\bar{Q}(\bar{X}_D),\bar{X}_D) \le 0; \quad j = 1,\text{NCON} \tag{2}$$

$$\bar{X}_{D_{lower}} \le \bar{X}_D \le \bar{X}_{D_{upper}} \tag{3}$$

where F is the objective function, NCON is the number of constraints, and Q is the vector of the conserved variables of the fluid flow. $\bar{X}_{D_{lower}}$ and $\bar{X}_{D_{upper}}$

are the lower and the upper bounds of the design variables. A judicious choice of the upper and lower bounds for the design variables accelerates convergence of the optimum solution. A fixed nozzle length, a fixed cowl thickness, and a fixed nozzle inlet height are imposed as the geometric constraints.

The axial component of the thrust force due to nozzle wall shape, F_{axial}, is obtained by integrating numerically the pressure over the ramp and cowl surfaces.

$$F_{axial} = \int_k^l P_{ramp} dy + \int_m^n P_{cowl} dy \tag{4}$$

This force is normalized by the force associated with the inflow given by

$$F_{inflow} = \int_k^c P_{th}(1 + \gamma M_{th}^2) dy \tag{5}$$

In the case of an inflow parallel to the cowl with a constant Mach number, this force is centered at the mid-point of the line segment $\overline{kc}$, and its value is

$$F_{inflow} = P_{th}(1 + \gamma M_{th}^2) H_{th} \tag{6}$$

By definition, the axial thrust force coefficient is given by

$$F = \frac{F_{axial}}{F_{inflow}} \tag{7}$$

This axial thrust force coefficient is subject to the following three constraints (i.e., NCON = 3):

1. The static pressure at the ramp tip, P_l, is forced to reach a percentage C_1, of the freestream static pressure, P_∞, such that a maximum expansion is reached without any back flow, i.e.

$$G_1(\bar{X}_D) = 1 - \frac{P_l}{C_1 P_\infty} \leq 0 \tag{8}$$

2. The static pressure at the cowl tip, P_n, should be within specified limits, (C_2 and C_3), of the freestream static pressure, P_∞, such that a maximum expansion is reached without any back flow on either of the cowl surfaces, i.e.

$$G_2(\bar{X}_D) = 1 - \frac{P_n}{C_2 P_\infty} \leq 0 \tag{9}$$

$$G_3(\bar{X}_D) = \frac{P_n}{C_3 P_\infty} - 1 \leq 0 \tag{10}$$

The derivatives of the objective function, F, and constraints G_j, with respect to the design variables, $\bar{X}_D$, are given by

$$\nabla F = \frac{dF}{d\bar{X}_D} = \frac{\partial F}{\partial \bar{X}_D} + \left(\frac{\partial F}{\partial \bar{Q}}\right)^T \frac{\partial \bar{Q}}{\partial \bar{X}_D} \tag{11}$$

$$\nabla G_j = \frac{dG_j}{d\bar{X}_D} = \frac{\partial G_j}{\partial \bar{X}_D} + \left(\frac{\partial G_j}{\partial \bar{Q}}\right)^T \frac{\partial \bar{Q}}{\partial \bar{X}_D} \qquad j = 1, NCON \tag{12}$$

Two different quasi-analytical approaches are available for obtaining these derivatives, the direct method, shown in figure 2, and the adjoint variable method, shown in figure 3. The choice of the particular sensitivity analysis approach depends on the number of design variables (NDV) and adjoint vectors (NCON+1). If the number of design variables is less than the number of adjoint vectors, the direct method is more efficient than the adjoint variable method. In the present example, the number of design variables (NDV = 2) is less than the number of adjoint vectors (NCON+1 = 4), the direct method is selected to determine the sensitivity coefficients.

The governing equations for two-dimensional, steady, compressible, inviscid flow of an ideal gas with constant specific heat ratios written in the residual vector form are

$$\bar{R}(\bar{Q}(\bar{X}_D),\bar{X}_D) = \frac{\partial \hat{f}}{\partial \xi} + \frac{\partial \hat{g}}{\partial \eta} = 0 \tag{13}$$

where $\hat{f}$ and $\hat{g}$ are the flux Jacobians in generalized coordinates (ξ, η).

The quasi-analytical direct method begins with the differentiation of Equation (13) with respect to the design variables to yield the sensitivity equation:

$$\left[\frac{\partial \bar{R}}{\partial \bar{Q}}\right] \left\{\frac{\partial \bar{Q}}{\partial \bar{X}_D}\right\} = -\left[\frac{\partial \bar{R}}{\partial \bar{X}_D}\right] \tag{14}$$

Then Equation (14) is solved for $\partial\bar{Q}/\partial\bar{X}_D$. Equation (14) needs to be solved once for each design variable $\bar{X}_D$, however, the coefficient matrix $(\partial\bar{R}/\partial\bar{Q})$ needs to be factorized once and for all. The remaining partial derivatives in Equations (11) and (12) are evaluated analytically using Equations (7-10). The final step is determining the values of ∇F and ∇G_j.

In order to reduce the number of CFD analyses during the optimization process, an approximate flow analysis is performed, which is based on a Taylor-series expansion of the vector of conserved variables $\bar{Q}(\bar{X}_D^* + \Delta\bar{X}_D)$ about $\bar{Q}(\bar{X}_D^*)$ as follows:

$$\bar{Q}(\bar{X}_D^* + \Delta\bar{X}_D) - \bar{Q}(\bar{X}_D^*) + \left(\frac{\partial \bar{Q}}{\partial \bar{X}_D}\right)_{\bar{X}_D - \bar{X}_D^*} \Delta\bar{X}_D + \ldots$$

(15)

Substituting Equation (14) into Equation (15) results in,

$$\left[\frac{\partial \bar{R}(\bar{Q}(\bar{X}_D^*), \bar{X}_D^*)}{\partial \bar{Q}}\right] \Delta\bar{Q} = -\left[\frac{\partial \bar{R}(\bar{Q}(\bar{X}_D^*), \bar{X}_D^*)}{\partial \bar{X}_D}\right] \Delta\bar{X}_D$$

(16)

where $\Delta\bar{Q} = \bar{Q}(\bar{X}_D^* + \Delta\bar{X}_D) - Q(\bar{X}_D^*)$.

Equation (16) gives the changes in $\bar{Q}$ due to the changes in $\Delta\bar{X}_D$. In other words, given the flow field solution, $\bar{Q}(\bar{X}_D^*)$, associated with a configuration, $\bar{X}_D^*$, the flow field solution $\bar{Q}(\bar{X}^* + \Delta\bar{X}_D)$, associated with the configuration, $(\bar{X}_D^* + \Delta\bar{X}_D)$, is obtained via Equation (16).

Although, the approximate analysis is less accurate than the actual analysis, it is less costly in terms of computer time, especially, when the number of flow field governing equations is large. However, the approximate analysis is of acceptable accuracy up to ±5% changes in the design variables.

Equation (13) is solved by a first-order accurate, implicit, upwind finite volume scheme. An upwind discretized form of Equation (13) at an interior cell (i,j) is as follows:

$$\begin{aligned}\bar{R}_{i,j} = {} & \hat{f}^{+}(\bar{Q}^{-}_{i+1/2,j}, M_{i+1/2,j}) - \hat{f}^{+}(\bar{Q}^{-}_{i-1/2,j}, M_{i-1/2,j}) \\ & + \hat{f}^{-}(\bar{Q}^{+}_{i+1/2,j}, M_{i+1/2,j}) - \hat{f}^{-}(\bar{Q}^{+}_{i-1/2,j}, M_{i-1/2,j}) \\ & + \hat{g}^{+}(\bar{Q}^{-}_{i,j+1/2}, M_{i,j+1/2}) - \hat{g}^{+}(\bar{Q}^{-}_{i,j-1/2}, M_{i,j-1/2}) \\ & + \hat{g}^{-}(\bar{Q}^{+}_{i,j+1/2}, M_{i,j+1/2}) - \hat{g}^{-}(\bar{Q}^{+}_{i,j-1/2}, M_{i,j-1/2})\end{aligned} \tag{17}$$

where $\hat{f}^{+}$, $\hat{f}^{-}$, $\hat{g}^{+}$, and $\hat{g}^{-}$ are the operator-split inviscid fluxes. M represents the projected surface areas for these fluxes and it is associated with the coordinate transformation metrics. The $\bar{Q}^{+}_{i+1/2,j}$ and $\bar{Q}^{-}_{i+1/2,j}$ for a first-order accurate scheme are given by,

$$\begin{aligned}\bar{Q}^{-}_{i+1/2,j} &= \bar{Q}_{i,j} \\ \bar{Q}^{+}_{i+1/2,j} &= \bar{Q}_{i+1,j}\end{aligned} \tag{18}$$

Consequently, the left-hand side of Equation (14) is evaluated by differentiating the upwind discretized form given by Equation (17) for an interior cell (i,j) with respect to $(Q^{\pm}_{i\pm1/2,j\pm1/2})$ as follows,

$$\begin{aligned}\left[\left\{\frac{\partial \bar{R}}{\partial \bar{Q}}\right\}\left\{\frac{\partial \bar{Q}}{\partial \bar{X}}\right\}\right]_{i,j} = {} & \frac{\partial \bar{R}_{i,j}}{\partial \bar{Q}^{-}_{i+1/2,j}}\frac{\partial \bar{Q}^{-}_{i+1/2,j}}{\partial \bar{X}_D} + \frac{\partial \bar{R}_{i,j}}{\partial \bar{Q}^{-}_{i-1/2,j}}\frac{\partial \bar{Q}^{-}_{i-1/2,j}}{\partial \bar{X}_D} \\ & + \frac{\partial \bar{R}_{i,j}}{\partial \bar{Q}^{+}_{i+1/2,j}}\frac{\partial \bar{Q}^{+}_{i+1/2,j}}{\partial \bar{X}_D} + \frac{\partial \bar{R}_{i,j}}{\partial \bar{Q}^{+}_{i-1/2,j}}\frac{\partial \bar{Q}^{+}_{i-1/2,j}}{\partial \bar{X}_D} \\ & + \frac{\partial \bar{R}_{i,j}}{\partial \bar{Q}^{-}_{i,j+1/2}}\frac{\partial \bar{Q}^{-}_{i,j+1/2}}{\partial \bar{X}_D} + \frac{\partial \bar{R}_{i,j}}{\partial \bar{Q}^{-}_{i,j-1/2}}\frac{\partial \bar{Q}^{-}_{i,j-1/2}}{\partial \bar{X}_D} \\ & + \frac{\partial \bar{R}_{i,j}}{\partial \bar{Q}^{+}_{i,j+1/2}}\frac{\partial \bar{Q}^{+}_{i,j+1/2}}{\partial \bar{X}_D} + \frac{\partial \bar{R}_{i,j}}{\partial \bar{Q}^{+}_{i,j-1/2}}\frac{\partial \bar{Q}^{+}_{i,j-1/2}}{\partial \bar{X}_D}\end{aligned} \tag{19}$$

Denoting the flux Jacobians by A and B, Equation (19) can be rewritten as,

$$\left[\left\{\frac{\partial \bar{R}}{\partial \bar{Q}}\right\}\left\{\frac{\partial \bar{Q}}{\partial \bar{X}_D}\right\}\right]_{IJ} = A^+_{IJ}\frac{\partial \bar{Q}^-_{I+1/2,J}}{\partial \bar{X}_D} - A^+_{I-1}\frac{\partial \bar{Q}^-_{I-1/2,J}}{\partial \bar{X}_D} + A^-_{I+1}\frac{\partial \bar{Q}^+_{I+1/2,J}}{\partial \bar{X}_D} - A^-_{IJ}\frac{\partial \bar{Q}^+_{I-1/2,J}}{\partial \bar{X}_D} + B^+_{IJ}\frac{\partial \bar{Q}^-_{IJ+1/2}}{\partial \bar{X}_D} - B^+_{IJ-1}\frac{\partial \bar{Q}^-_{IJ-1/2}}{\partial \bar{X}_D} + B^-_{IJ+1}\frac{\partial \bar{Q}^+_{IJ+1/2}}{\partial \bar{X}_D} - B^-_{IJ}\frac{\partial \bar{Q}^+_{IJ-1/2}}{\partial \bar{X}_D} \tag{20}$$

The values of the conserved variables at the cell-interface locations $(\bar{Q}^{\pm}_{I\pm1/2,J\pm1/2})$ can be viewed as functions of the values of the conserved variables of the neighboring cells evaluated at the centers. Therefore, the terms $[\partial\bar{Q}^{\pm}_{I\pm1/2,J}/\partial\bar{X}_D]$ and $[\partial\bar{Q}^{+}_{I,J\pm1/2}/\partial\bar{X}_D]$ in Eq. (20) can be expressed in terms of $[\partial\bar{Q}_{I\pm1,J}/\partial\bar{X}_D]$, $[\partial\bar{Q}_{I,J}/\partial\bar{X}_D]$, and $[\partial\bar{Q}_{I,J\pm1}/\partial\bar{X}_D]$. Hence, Eq. (20) is rewritten as

$$\left[\left\{\frac{\partial \bar{R}}{\partial \bar{Q}}\right\}\left\{\frac{\partial \bar{Q}}{\partial \bar{X}_D}\right\}\right]_{IJ} = A^+_{I-1}\frac{\partial \bar{Q}_{I-1,J}}{\partial \bar{X}_D} + (A^+_{IJ}+B^+_{IJ}+A^-_{IJ}+B^-_{IJ})\frac{\partial \bar{Q}_{IJ}}{\partial \bar{X}_D} + A^-_{I+1}\frac{\partial \bar{Q}_{I+1,J}}{\partial \bar{X}_D} + B^+_{IJ-1}\frac{\partial \bar{Q}_{IJ-1}}{\partial \bar{X}_D} + B^-_{IJ+1}\frac{\partial \bar{Q}_{IJ+1}}{\partial \bar{X}_D} \tag{21}$$

The coefficients $\bar{A}$ through $\bar{E}$ in Equation (21) are 4x4 blocks which are functions of the flux Jacobians $A^{\pm}$ and $B^{\pm}$. These flux Jacobians $A^{\pm}$ and $B^{\pm}$ are usually available for an interior cell from the flowfield solution when forcing the residual to zero. Hence, only a few computations are needed to assemble the

Jacobian matrix $[\partial\bar{R}/\partial\bar{Q}]$ in Eq (14). However, it is necessary to revise the residual expression (Equation 17) at the boundary points to include the boundary conditions.

Once the numerical values of all the elements in the (n x n) coefficient matrix are obtained, the coefficient matrix can be assembled. It has a block banded structure with five nonzero computational domain with I cells in the ξ direction and J cells in the η direction, the matrix dimension, n, is (4IJ). The first order upwind discretization of the governing equations yields a coefficient matrix with a subdiagonal bandwidth of (4J + 3) or (4I + 3), depending on the way in which the unknowns are ordered. The diagonal storage of band matrices and the unknown ordering resulting in the minimum bandwidth are used in the present example to reduce the computer memory requirement.

The right-hand side of Equation (14) is evaluated by differentiating Equation (17) for an interior cell (i,j) with respect to the design variables, $\bar{X}_D$, as follows,

$$\frac{\partial \bar{R}_{IJ}}{\partial \bar{X}_D} = \left[\frac{\partial \hat{f}^+(\bar{Q}^-_{I+1/2,J}, M_{I+1/2,J})}{\partial(M_{I+1/2,J})} + \frac{\partial \hat{f}^-(\bar{Q}^+_{I+1/2,J}, M_{I+1/2,J})}{\partial(M_{I+1/2,J})}\right]\frac{\partial(M_{I+1/2,J})}{\partial \bar{X}_D}$$
$$- \left[\frac{\partial \hat{f}^+(\bar{Q}^-_{I-1/2,J}, M_{I-1/2,J})}{\partial(M_{I-1/2,J})} + \frac{\partial \hat{f}^-(\bar{Q}^+_{I-1/2,J}, M_{I-1/2,J})}{\partial(M_{I-1/2,J})}\right]\frac{\partial(M_{I-1/2,J})}{\partial \bar{X}_D}$$
$$+ \left[\frac{\partial \hat{g}^+(\bar{Q}^-_{I,J+1/2}, M_{I,J+1/2})}{\partial(M_{I,J+1/2})} + \frac{\partial \hat{g}^-(\bar{Q}^+_{I,J+1/2}, M_{I,J+1/2})}{\partial(M_{I,J+1/2})}\right]\frac{\partial(M_{I,J+1/2})}{\partial \bar{X}_D}$$
$$- \left[\frac{\partial \hat{g}^+(\bar{Q}^-_{I,J-1/2}, M_{I,J-1/2})}{\partial(M_{I,J-1/2})} + \frac{\partial \hat{g}^-(\bar{Q}^+_{I,J-1/2}, M_{I,J-1/2})}{\partial(M_{I,J-1/2})}\right]\frac{\partial(M_{I,J-1/2})}{\partial \bar{X}_D} \tag{22}$$

As it is seen from Equation (22), $[\partial\bar{R}/\partial\bar{X}_D]$ depends on the derivatives of the projected surface areas (M) with respect to the design variables. If an analytical expression for $M = M(\bar{X}_D)$ exists, then this differentiation is

straightforward. Otherwise, a finite difference approximation for $\partial M/\partial \bar{X}_D$ with a small step size $\Delta \bar{X}_D$ can be used.

Finally, the solution of the system of linear algebraic equations (14) is achieved by using the Gauss elimination method on the elements within the bandwidth only.

The computational fluid dynamics analyses are performed using the general purpose, finite volume Euler/Navier-Stokes CFD code "VUMXZ3". This code has been applied to analyze a variety of complex internal and external flows. It produces consistent and repeatable flow simulations in the sense that small perturbations to design variables are accurately reflected in the flowfield solution.

A key part of the present design procedure is the sensitivity analysis where the derivatives of the constraints, the objective function and the conserved flow variables, with respect to the design variables are computed. The derivatives quantify the effects of each design variable on the design and thereby identify the most important design changes to make enroute to the optimum design. Two different quasi-analytical approaches are available for obtaining these derivatives, the direct method, shown in figure 2 and the adjoint variable method, shown in figure 3. The choice of the particular sensitivity analysis approach depends on the number of design variables and adjoint vectors. If the number of design variables is greater than the number of adjoint vectors, the adjoint variable method is more efficient than the direct method.

The present nonlinear, constrained optimization problem is solved using the modified feasible directions method developed by Vanderplaats ("An Efficient Feasible Direction Algorithm for Design Synthesis," AIAA J., Vol. 22, No. 11, October, 1984, pp. 1633-1640). Given a set of initial conditions for design variables, the method first determines if the initial values are in the feasible design space, i.e., the space when none of the design constraints are violated. If not, then the design variables must be changed until the feasible

design space is located. At this point, the method can search to find the optimum design within the feasible design space.

Since the optimization process requires many evaluations of the objective function and constraints before an optimum design is obtained, the process can be very expensive if a CFD analysis were performed for each evaluation. However, the optimization process primarily uses analysis results to move in the direction of the optimum design. Hence an analysis needs to be made only occasionally during the design process and always at the end to check the final design. In the present process, approximate flow analyses using Equation 16 are performed through the one-dimensional search of the optimization process, whereas the CFD analysis is performed only when new gradients of constraints and objective function are needed, i.e. when the design changes substantially.

Finally the sensitivity information is passed to the optimizer along with the current values of the design variables, constraints, and the objective function. The optimizer uses this information to generate a new set of design variables and the entire procedure is repeated until a converged design is obtained. The design algorithm is deemed converged when all the constraints are satisfied and the objective function has a value which does not change for a specified number of optimization loops.

After the optimum design is obtained, it is desirable to determine the sensitivity of the optimum design with respect to one or more design parameters. Such information is useful to perform trade-off analyses. For example, it may be wished to estimate what effect a specified increase in the free stream Mach number has on the optimum thrust. Mathematically, this requires the derivatives of the optimum values of the objective function and the corresponding design variables with respect to the design parameters. In the present example, the design parameters are the specific heat ratio, γ, Mach numbers, total temperatures and total pressures of both the external flow and the internal flow leading to the nozzle jet.

The first-order sensitivity derivative method is adapted for the present invention. The vector $\bar{P}$ contains the design parameters, which are held fixed during the optimization. Using the superscript "op" to denote the optimum quantities, the dependence of F^{op} and G on $\bar{X}_D$ and $\bar{P}$ can be written as,

$$F^{op} = F^{op}(\bar{Q}(\bar{X}_D(\bar{P}),\bar{P}),\bar{X}_D(\bar{P}),\bar{P}) \tag{23}$$

$$\bar{G}_a = \bar{G}_a(\bar{Q}(\bar{X}_D(\bar{P}),\bar{P}),\bar{X}_D(\bar{P}),\bar{P}) = 0 \tag{24}$$

where $\bar{G}_a$ is a vector containing only the active constraints at the constrained maximum. The total optimum sensitivity derivative of the objective function with respect to a design parameter P is obtained using the chain rule of differentiation

$$\frac{dF^{op}}{dP} = \frac{\partial F^{op}}{\partial P} + \left[\left(\frac{\partial F^{op}}{\partial \bar{Q}}\right)^T \frac{\partial \bar{Q}}{\partial \bar{X}_D} + \frac{\partial F^{op}}{\partial \bar{X}_D}\right]^T \frac{\partial \bar{X}_D}{\partial P} + \left(\frac{\partial F^{op}}{\partial \bar{Q}}\right)^T \frac{\partial \bar{Q}}{\partial P} \tag{25}$$

Any perturbation of the parameter P about its value at the initial optimum must be such that the originally active constraints remain active,

$$\frac{d}{dP}\bar{G}_a - \frac{\partial \bar{G}_a}{\partial P} + \left[\left(\frac{\partial \bar{G}_a}{\partial \bar{Q}}\right)^T \frac{\partial \bar{Q}}{\partial \bar{X}_D} + \frac{\partial \bar{G}_a}{\partial \bar{X}_D}\right]^T \frac{\partial \bar{X}_D}{\partial P} + \left(\frac{\partial \bar{G}_a}{\partial \bar{Q}}\right)^T \frac{\partial \bar{Q}}{\partial P} = 0 \qquad (26)$$

The Kuhn-Tucker condition satisfied at a local optimum is

$$\left[\left(\frac{\partial F^{op}}{\partial \bar{Q}}\right)^T \frac{\partial \bar{Q}}{\partial \bar{X}_D} + \frac{\partial F^{op}}{\partial \bar{X}_D}\right] + \left[\left(\frac{\partial \bar{G}_a}{\partial \bar{Q}}\right)^T \frac{\partial \bar{Q}}{\partial \bar{X}_D} + \frac{\partial \bar{G}_a}{\partial \bar{X}_D}\right] \bar{\psi} = 0 \qquad (27)$$

where $\bar{\psi}$ is a vector containing the Lagrangian multipliers. Combining Eqs. (26) and (27) yields,

$$\left[\left(\frac{\partial F^{op}}{\partial \bar{Q}}\right)^T \frac{\partial \bar{Q}}{\partial \bar{X}_D} + \frac{\partial F^{op}}{\partial \bar{X}_D}\right]^T \frac{\partial \bar{X}_D}{\partial P} = -\bar{\psi}^T \left[\frac{\partial \bar{G}_a}{\partial P} + \left(\frac{\partial \bar{G}_a}{\partial \bar{Q}}\right)^T \frac{\partial \bar{Q}}{\partial P}\right] \qquad (28)$$

Equation (28) is put into Equation (25) in order to eliminate $\left(\frac{\partial \bar{X}_D}{\partial P}\right)$,

$$\frac{dF^{op}}{dP} - \frac{\partial F^{op}}{\partial P} + \bar{\psi}^T \frac{\partial \bar{G}_a}{\partial P} + \left[\left(\frac{\partial F^{op}}{\partial \bar{Q}}\right)^T + \bar{\psi}^T \left(\frac{\partial \bar{G}_a}{\partial \bar{Q}}\right)^T\right] \frac{\partial \bar{Q}}{\partial P} \qquad (29)$$

The Lagrangian multipliers in Equation (29) are obtained from the following relation evaluated at the optimum point

$$\bar{\psi} = -\left[(\nabla \bar{G}_j)^T \nabla \bar{G}_a\right]^{-1} \left[\nabla \bar{G}_a\right]^T \nabla F^{op} \tag{30}$$

The derivatives of the vector of conserved variables $\bar{Q}$ with respect to the design parameters are obtained as follows

$$\bar{R}(\bar{Q}(\bar{X}_D(\bar{P}),\bar{P}),\bar{X}_D(\bar{P}),\bar{P}) = 0 \tag{31}$$

Differentiation of Equation (31) with respect to the design parameters yields,

$$\frac{d\bar{R}}{d\bar{P}} = \frac{\partial \bar{R}}{\partial \bar{P}} + \left[\frac{\partial \bar{R}}{\partial \bar{X}_D} + \frac{\partial \bar{R}}{\partial \bar{Q}} \frac{\partial \bar{Q}}{\partial \bar{X}_D}\right]^T \frac{\partial \bar{X}_D}{\partial P} + \frac{\partial \bar{R}}{\partial \bar{Q}} \frac{\partial \bar{Q}}{\partial \bar{P}} = 0 \tag{32}$$

Using Equation (14) with Equation (32) results in,

$$\left[\frac{\partial \bar{R}}{\partial \bar{Q}}\right] \frac{\partial \bar{Q}}{\partial \bar{P}} = -\left[\frac{\partial \bar{R}}{\partial \bar{P}}\right] = \bar{R}_v \tag{33}$$

Solving Equation (33) similarly to Equation (14) for $\frac{\partial \bar{Q}}{\partial P}$ and substituting it into (29) yields the sensitivities of the objective function to the design parameters.

Since the number of design parameters (equal to seven to the present example) is greater than the number of the adjoint vectors (equal to one for the present example), the adjoint variable method, is more economical. This can be seen from the following substitution of Equation (33) into Equation (29).

$$\frac{dF^{op}}{dP} = \frac{\partial F^{op}}{\partial P} + \bar{\psi}^T \frac{\partial \bar{G}_a}{\partial P} + \left[\left(\frac{\partial F^{op}}{\partial \bar{Q}}\right)^T + \bar{\psi}^T \left(\frac{\partial \bar{G}_a}{\partial \bar{Q}}\right)^T\right] J^{-1} R_v \tag{34}$$

where $J^{-1} = \left[\frac{\partial \bar{R}}{\partial Q}\right]^{-1}$. Then, an adjoint vector $\bar{\lambda}$, that satisfies the following equation is defined,

$$J^T \bar{\lambda} = \left[\frac{\partial F^{op}}{\partial \bar{Q}} + \left(\frac{\partial \bar{G}_a}{\partial \bar{Q}} \bar{\psi}\right)\right] \tag{35}$$

Substitution of Equation (35) into Equation (34) gives

$$\frac{dF^{op}}{dP} = \frac{\partial F^{op}}{\partial P} + \bar{\psi}^T \frac{\partial \bar{G}_a}{\partial P} + \bar{\lambda}^T \bar{R}_v \tag{36}$$

The adjoint system of Equation (35) is independent of any differentiation with respect to the design parameters. Also, both terms on the right hand side of Equation (35) are available from the calculations of Eqs. (11) and (12). The

partial derivatives, $\frac{\partial F^{op}}{\partial P}$, $\frac{\partial \bar{G}_a}{\partial P}$ and $\frac{\partial R}{\partial P}$ are evaluated analytically. Therefore, the sensitivity derivatives (Equation 36) are obtained after solving Equation (35), evaluating Equation (30) and pertinent substitutions.

What is claimed is:

LAR 14815-1-CU PATENT APPLICATION

AERODYNAMIC DESIGN OPTIMIZATION USING SENSITIVITY ANALYSIS AND COMPUTATIONAL FLUID DYNAMICS

Abstract of the Disclosure

An efficient aerodynamic shape optimization method based on a computational fluid dynamics/sensitivity analysis algorithm has been developed which determines automatically the geometrical definition of an optimal surface starting from any initial arbitrary geometry. This method is not limited to any number of design variables or to any class of surfaces for the shape definition.

AERODYNAMIC DESIGN OPTIMIZATION FLOWCHART

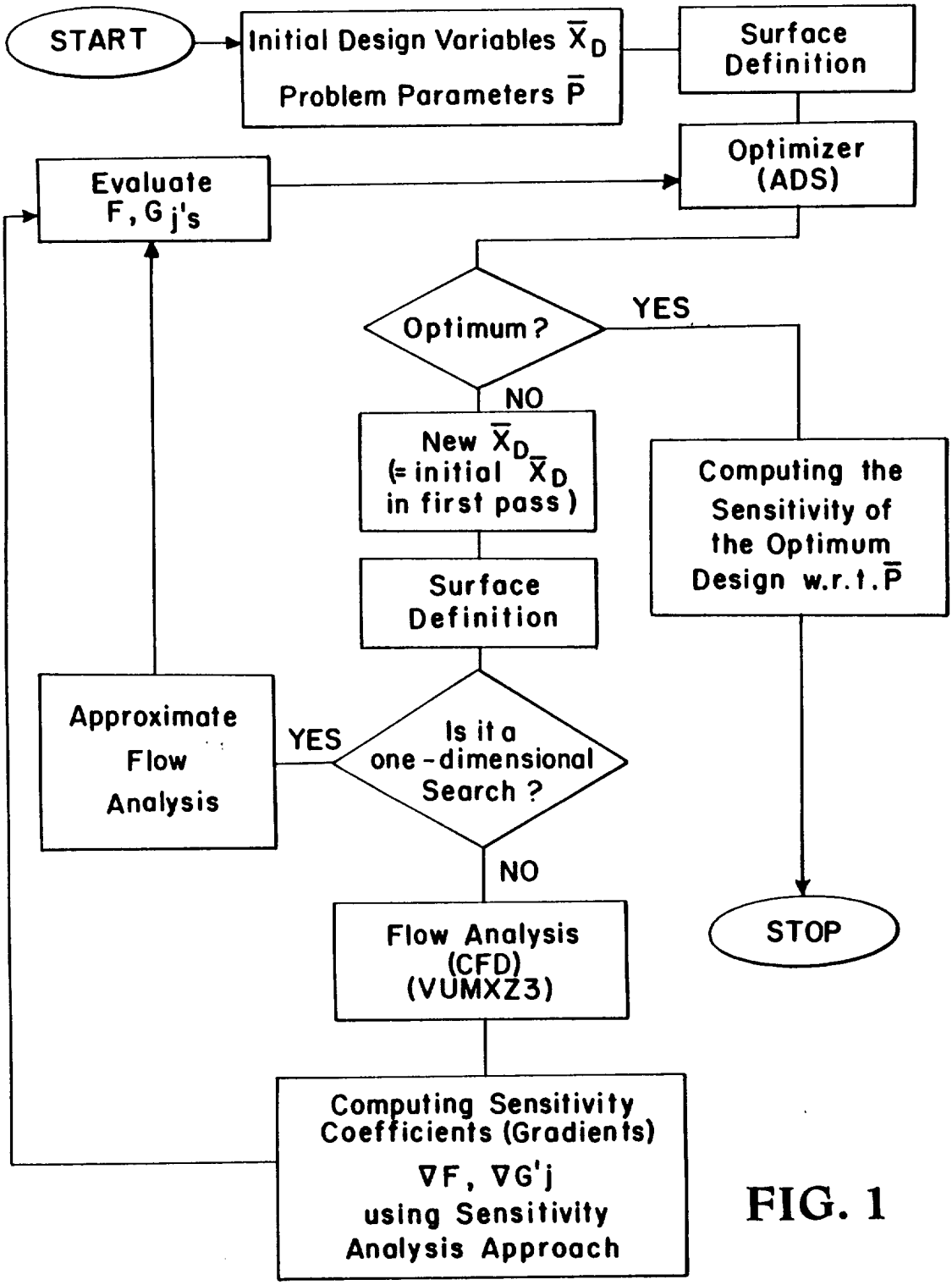

FIG. 1

I. DIRECT METHOD

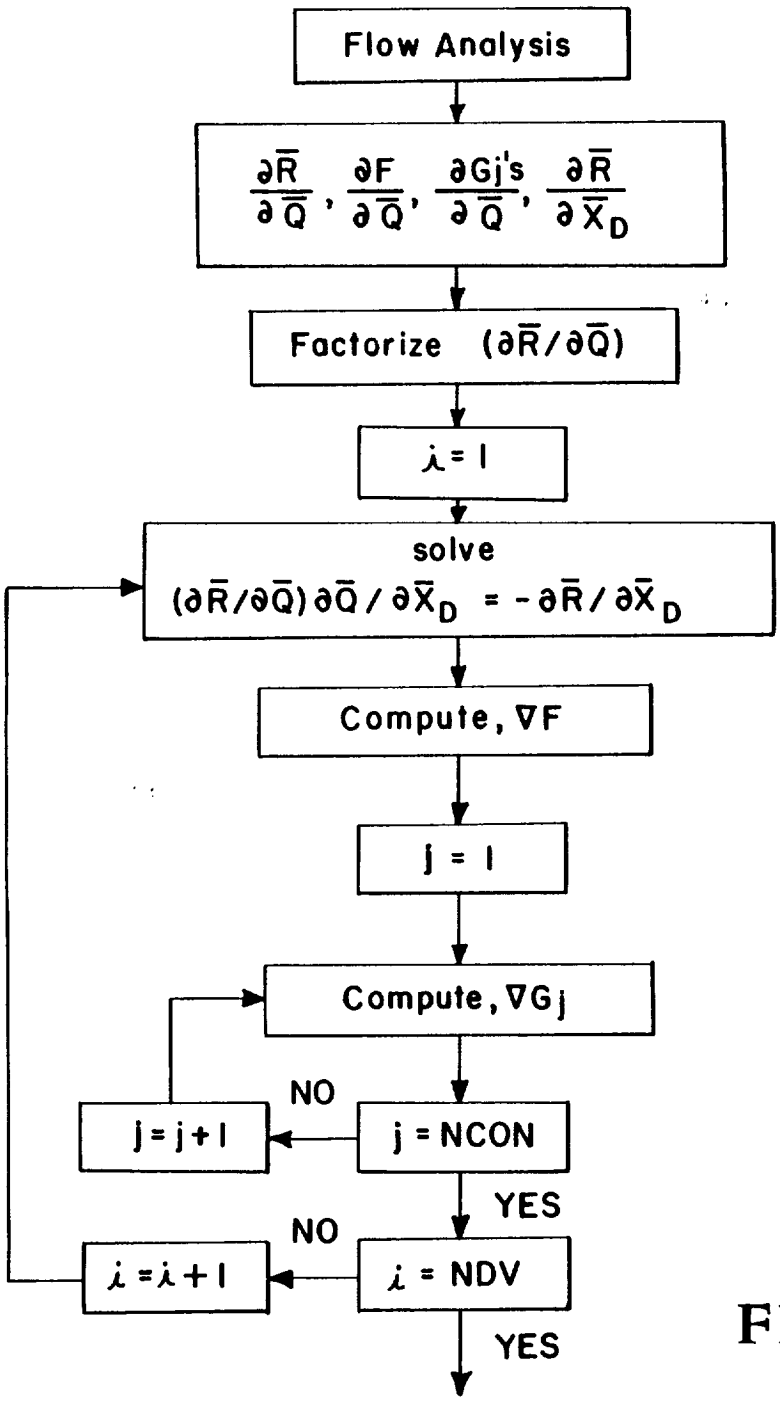

FIG. 2

II. ADJOINT VARIABLE METHOD

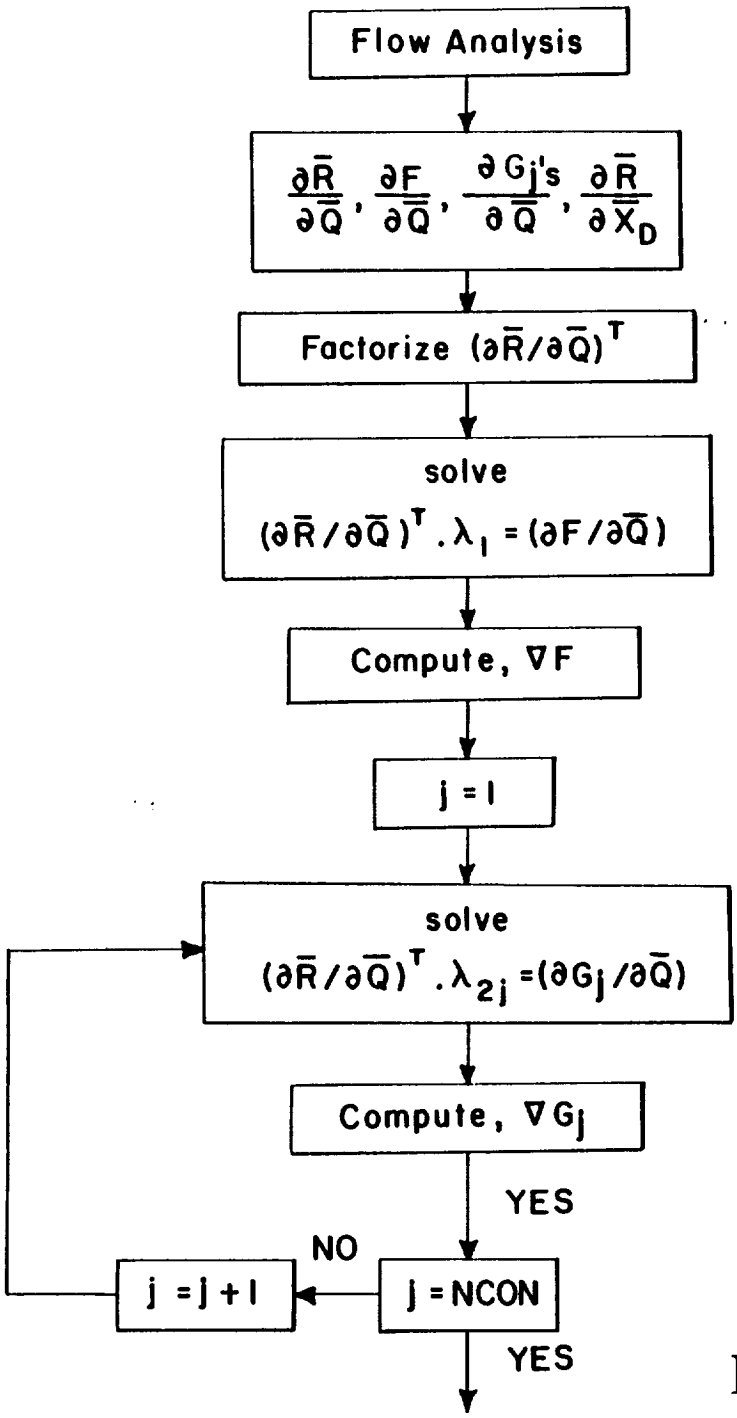

FIG. 3